Author Comments for Review #1

The authors are grateful for the comments, suggestions, and insight from the reviewer. The authors have made a significant effort to address all the comments below as we believe that not only is the question relevant, but the scientific quality is attainable given the work. We have revised the entire manuscript and believe it now surpasses the necessary scientific quality. Please find comments below [with text locations included where appropriate] and an updated version of the paper below.

RC1 The manuscript adresses a relevant scientific question within the scope of WES but does not fulfill scientific quality. I suggest to rejected the manuscript in its current version.

AR Significant revisions have been made and we respectfully request acceptance as we have addressed the reviewers' comments with this version.

RC2 Abstract: The abstract is fluffy and does not clearly state the work/scientific contribution. First the introduction shed some light on the work. The abstract does not provide a concise and complete summary and neither includes quantitative results.

AR Thank you for this comment. The abstract has been re-written to address these concerns. In particular, it has been re-written to focus on the scope of the content, and to orient the reader for expectations from the work.

RC3 Introduction: The introduction states the work tasks: Flaw characterization and effects of defects. The introduction does not give proper credit to related and relevant work in this area and does not at all quote any related work in the field of progressive damage in composites related to manufacturing induced waves beside from self-citations.

AR The introduction has been significantly modified to more clearly state the purpose and goal of this work. Additional references have been added throughout to cite the significant contributions of others. Given that the breadth of work in this area, the focus has been on foundational and influential works.
Finally, the authors believe that the self-reference noted has been misconstrued as it refers to the companion paper that has been submitted with this paper that outlines the significant experimental work supporting the work presented here. Clarity of the importance of this companion paper and its distinction has been reinforced in the introduction, methods, and results.

RC4 The differentiation between CDM and DDM is not clearly described. Furthermore, section 1.1 and 1.2 are textbook like copy-paste paragraphs from probably the PhD thesis and are not suited for a scientific article.

AR These sections have been re-written to clearly define these techniques, emphasize the differences, and highlight the state of the art in these fields. Further clarifications have been made in the Conclusions and Future Work section.

RC5 Section 3: Modelling Techniques: The section is very fluffy. The boundary conditions are not stated, instead referred to experimental work that is not described at all. The tables 1 and 2 are of bad quality.

AR The entire section has been reworked to identify the methods used and allow for recreation of the work described. Tables 1 and 2 have both been improved with additional descriptions and Figure 1 has been updated as well. [Note that this is now Section 2] Details and actual code have been added to provide the reader with all information necessary to reproduce the work if desired.

RC6 Section 3.1 is a complete copy of the Abaqus manual.

AR While the first sentence of this section continues to be a direct reference to this fact, the section has been truncated and the reader is referenced to Abaqus as needed. Only what is need to recreate the work is included. [Note that this is now Section 2.1] In particular, this is necessary to show the reader how different failure modes were modeled, and how the progressive damage with the Hashin model fits in with the Continuum Damage Modeling described in the paper.

RC7 Section 3.2 is ok, but does not really describe the user-defined subroutine well.

AR Additional clarity of the subroutine and user-defined failure criteria have been added. [Note that this is now Section 2.2]

RC8 Section 3.4 Cohesive Zone Model. The statement "While previous convention was to utilize cohesive elements only in specific areas, pre-defining the crack path, computation availability has made it conceivable to place cohesive elements throughout the model. Thus, damage and crack progression may occur virtually anywhere in the model where the stress state indicates rather than where the user has placed these elements." is not correct. The damage and crack progression can still only occur where cohesive elements are placed. And since two cohesive elements cannot be connected and crack growth is limited to one direction, cracks can still only propagate inside the cohesive elements and not crack unification is possible.

AR The authors understand the spirit of this comment and agree that our original statement is beyond the work described in here. Our group and others have made significant progress in development of intrinsic cohesive zone models where MPC's are selectively released allowing crack initiation and growth as described by the quoted statement above (https://dx.doi.org/10.4236/jamp.2014.212121). However, given that this is not descriptive of the work herein, we have chosen to reword these statements [now Section 2.4, p 12, lines 6-9]. Since the crack paths are generally known to be between fiber tows, the models herein have all of these potential paths (between every row of fibers) modeled at once instead of just a few given advances in computational availability. Further clarification is provided. "It is important to note that the damage does not necessarily occur at the cohesive zone area. It only provides the opportunity for growth where damage can, and has been experimentally determined to grow before final failure. Damage growth only occurs when and where the critical load is met. This is an important distinction from assuming a damage path as in the case of conventional Linear Elastic Fracture Mechanics."

Author Comments for Review #2

The authors are grateful for the comments, suggestions, and insight from the reviewer. The authors have made a significant effort to address all the comments below as we believe that not only is the question relevant, but the scientific quality is attainable given the work. We have revised the entire manuscript and believe it now surpasses the necessary scientific quality. Please find comments below [with text locations included where appropriate] and an updated version of the paper below.

RC1 Overall, the writing is appreciated and the work contributes to a relevant area, however significant revisions should be made to the reporting of the work prior to being acceptable for publication.

AR Significant revisions have been made and we respectfully request acceptance of this major revision

RC2 The abstract should be rewritten with a more specific focus on the stated goal / hypothesis of the work and the conclusions clearly stated.

Thank you for this comment. The abstract has been re-written with these comments in mind. In particular, it has been re-written to focus on the scope of the content, and to orient the reader for expectations from the work.

RC3 The introduction does not give proper credit to other research ongoing in the field and a more extensive literature review should be performed.

AR The introduction has been significantly modified to more clearly state the purpose and goal of this work. Additional references have been added throughout to cite the significant contributions of others. Given that the breadth of work in this area, the focus has been on foundational and influential works. The original manuscript included only foundational work, but other complementary work has been added for completeness.

RC4 Boundary conditions of the models are not discussed yet are necessary for comparison to any experimental data, as well as for replication of the study.

AR The entire section has been reworked to identify the methods used and allow for recreation of the work described. Tables 1 and 2 have both been improved with additional descriptions and Figure 1 has been updated as well. [Note that this is now Section 2] As for the experimental work, a companion paper has been submitted with this paper that outlines the significant experimental work supporting the work presented here. Clarity of the importance of this companion paper, and reference to it, has been reinforced in the introduction, methods, and results.

RC5 There is no discussion of the test which is performed for validation. This should at least be touched on so it can be discussed within the context of the paper. I'm not sure what is being "compared" in figure 6. There is no scales or legends, and no actual data is shown for the experimental results. Perhaps this figure could be augmented to more clearly demonstrate what the author is trying to discuss.

AR The entirety of what is now Section 3 [formerly Section 2] is a discussion of the validation test approach. It ties together the experimental data with the method of validation and what was considered acceptable modification of each model. This more effectively leads into the results and in particular sets up Table 6 [formerly Table 4] and Figure 9 [formerly Figure 6]. Figure 6 has been reworked to more clearly show the correlations between the analytical and experimental work. Legends are not given for the strain fields of the analytical results because the authors believe they misrepresent the correlation. Instead a visual inspection shows similar damage progression. Addition of both stress-strain responses allows the reader to see not only the full-field average strain at these two points, but for entire loading. The authors appreciate this comment as it has led to this better explanation.

RC6 No results are shown of testing other than the IP wave model. How did the other models compare with respect to OP models. No data is really talked about with respect to Porosity. If no models were run, why discuss it? If so, discuss the results.

AR Specifics have been added for Porosity [Section 4.1], OP Waves [4.3], and additional waves [4.4] falling in line with expansion of results/discussion to deal with validation, tuning, etc.

Progressive Damage Modelling of Fiberglass/Epoxy Composites with Manufacturing Induced Waves Common to Wind Turbine Blades

Jared W. Nelson[1], Trey W. Riddle[2], and Douglas S. Cairns[3]

[1]SUNY New Paltz, Division of Engineering Programs, New Paltz, NY USA
[2]Sunstrand, LLC, Louisville, KY USA
[3]Montana State University, Dept. of Mechanical and Industrial Engineering, Bozeman, MT USA

Abstract. Composite wind turbne blades are typically reliable.; Hhowever, premature failures are often in regions of manufacturing defects. While the use of damage modelling has increased with improved computational capabilities, they are often performed for worst-case scenarios where damage or defects are replaced with notches or holes. To better understand and predict these effects, an effects of defects study has been undertaken. As a portion of this study, various progressive damage modelling approaches were investigated to determine if sufficient modelling capabilities existed to predict damage progression of composite laminates with typical manufacturing flawes included. ~~While the use of damage modelling has increased with improved computational capabilities, they are often performed for worst-case scenarios where damage or defects are replaced with notches or holes. To contribute to the establishment of a protocol understanding and quantifying the effects of these defects, a three round study was performed using continuum, discrete, and combined damage modelling. This approach relied on~~ Models were constructed to match the coupons from, and compare the results to, the characterization and material testing study presented as a companion. Modelling types included a linear elastic with Hashin failure criteria, user-defined failure criteria, non-linear shear criteria, cohesive elements, and a combined non-linear shear with cohesive elements. ~~a~~A systematic, combined qualtitative/quantitative approach was used to ~~ally~~ compare~~ing~~ consistency, accuracy and predictive capability for each model to responses found experimentally. ~~These models were constructed to match the coupons from, and compare the results to, the characterization and material testing study. A standard defect case was chosen and initially used for each modelling approach to perform the qualitative and quantitative comparisons.~~ Results indicated that the Hashin and combined models were best able to predict material response in most cases while the rest did not correlate. ~~It was found that while each model was able to show certain attributes, the most consistent, accurate, and predictive model was based on a combined continuum/discrete method.~~ Overall, the results indicate that this combined approach may provide insight into blade performance with known defects when used in conjunction with a probabilistic flaw framework.

1 Introduction

The US Department of Energy sponsored, Sandia National Laboratory led, Blade Reliability Collaborative (BRC) has been tasked with developing a comprehensive understanding of wind turbine blade reliability (Paquette, 2012).

A major component of this task is to characterize, understand, and predict the effects of manufacturing flaws commonly found in blades. Building upon coupon testing, outlined in the companion paper (Nelson et al., 2017), which determined material properties and characterized damage progression, three composite material defect types were investigated: porosity, in-plane (IP) waviness, and out-of-plane (OP) waviness. These defects were identified by an industry Delphi group as being common and deleterious to reliability (Paquette, 2012). Significant research into effects of common composite laminate defects has been performed for both porosity (Wisnom et al., 1996; Baley et al., 2004; Costa et al., 2005; Huang and Talreja, 2005; Pradeep et al., 2007; Zhu et al., 2009; Guo et al., 2009) and fiber waviness (Adams and Bell, 1995; Adams and Hyer, 1996; Cairns et al., 1999; Niu and Talreja, 1999; Avery et al., 2004; Wang et al., 2012; Lemanski et al., 2013; Mandell and Samborsky, 2013). The goal of this portion of the overall project was to establish analytical approaches to model progressive damage in flawed composite laminates consistently and accurately predict laminate response. Multiple cases for each flaw type were tested allowing for progressive damage quantification, material property definition, and development of many correlation points in this work. As outlined in the following sections, there have been two primary modelling approaches used to assess damage progression in composite laminates: Continuum Damage Modelling (CDM), and Discrete Damage Modelling (DDM). While these methods are well established, there has been little work directly assessing predictive capabilities when applied to wind turbine blade laminates with defects.

~~A major component of this task is to characterize and understand manufacturing flaws commonly found in blades. In this paper, the authors describe and develop two tasks; Flaw Characterization and Effects of Defects. Characterizing flaws is necessary to determine and quantify what manufacturing defects are present. The Effects of Defects is focused on understanding the mechanical performance of materials containing typical flaws and comparing various progressive damage models techniques. Different analytical approaches to model progressive damage in flawed composite laminates for consistency, accuracy, and predictive capability were developed and evaluated.. Building upon coupon testing which determined material properties and characterized damage progression, three composite material defect types were investigated: in-plane (IP) waviness, out-of-plane (OP) waviness, and porosity (Nelson et al., 2017). Multiple cases for each flaw type were tested allowing for progressive damage quantification, material property definition, and development of many correlation points in this work.~~

1.1 Continuum Damage Modelling Background

~~Two distinct modelling methods have been investigated and compared: Continuum Damage Modelling (CDM), and Discrete Damage Modelling (DDM) (Nelson et al., 2012; Woo et al, 2013).~~ Continuum Damage Modelling (CDM) is a "pseudo-representation" that does not explicitly model the exact damage but instead, updates the constitutive properties as damage

occurs (Kachanov, 1986). ~~This approach assumes that a material is continuous and fills an entire region of space. From this region, the material is broken into representative volume element (RVE) unit cells such that constitutive equations relate the RVE to the entire structure.~~ This allows for the relating of equations to heterogeneous micro-processes that occur during strain of materials locally, and during strain of structures globally, insofar as they are to be described by global continuum variables given their non-homogeneity (Talreja, 1985; Chaboche, 1995). ~~Simply put, actual description of damage is difficult, especially when the damage is on a grain, cell, or micro scale; however, a change in global material response is rather easily noted from the onset of damage. As such, it is often useful to homogenize the material properties of the RVE, a process which is not always feasible when studying composites. In some instances, the two different materials cannot be represented accurately in such a way, especially when damage occurs independently in one of the constituents. Thus, care must be given to the failure modes and types when accounting for the changes in constitutive properties through the damage phases.~~

Thus, for typical CDM as the model iterates at each strain level, the constitutive matrix is updated to reflect equilibrium damage. Then as damage occurs, the elastic properties are irreversibly affected in ways that are similar to those in a general framework of an irreversible thermodynamic process (Kachanov, 1986). ~~As shown in Figure 1, t~~This may take~~s~~ place by reducing the elastic properties (E_1, E_2, ν_{12}, ν_{32}, and G_{12}) in the stiffness matrix (C) of the stress-strain relationship. Damage is not directly measurable from this approach, but may be estimated for the continuum by altering observable properties: strength, stiffness, toughness, stability, and residual life. ~~While this method is simple, in some instances two different materials cannot be represented accurately this way and care must be given to the failure modes and types when accounting for the changes in constitutive properties.~~

$$\begin{Bmatrix}\sigma_{xx}\\ \sigma_{yy}\\ \sigma_{zz}\\ \sigma_{yz}\\ \sigma_{zx}\\ \sigma_{xy}\end{Bmatrix} = \begin{Bmatrix} C_{11} & C_{12} & C_{13} & 0 & 0 & 0 \\ & C_{11} & C_{13} & 0 & 0 & 0 \\ & & C_{33} & 0 & 0 & 0 \\ & & & C_{44} & 0 & 0 \\ & sym & & & C_{44} & 0 \\ & & & & & (C_{12}-C_{12})/2 \end{Bmatrix} \begin{Bmatrix}\varepsilon_{xx}\\ \varepsilon_{yy}\\ \varepsilon_{zz}\\ \varepsilon_{yz}\\ \varepsilon_{zx}\\ \varepsilon_{xy}\end{Bmatrix}$$

~~**Figure 1: Stress-strain relation for a transversely isotropic laminate where the stiffness matrix, *C*, is made up of five elastic constants: E_1, E_2, ν_{12}, ν_{32}, and G_{12}.**~~

~~**1.1 Continuum Damage Modelling Background**~~

~~Continuum approaches for composite materials have been well established (Blacketter et al., 1993; Chapman and Whitcomb, 2000; Gorbatikh et al., 2007). In some cases, finite element analysis has been used to account independently for fiber and matrix damage. Chang and Chang (1987) developed a composite laminate in tension with a circular hole where material properties were degraded to represent damage. Failure criteria were defined based on the failure mechanisms resulting from damage: matrix cracking, fiber-matrix shearing, and fiber breakage. A property reduction model was implemented and the results were in agreement for seven (7) independent laminates. Later,~~ Damage may be viewed as the creation of discontinuities, and Kachanov (1986) suggested a single scalar variable as a measure of the effective surface density of these discontinuities. This approach assumes that load redistribution to undamaged areas or ligaments occurs, and effective stresses increase, until

all ligaments are severed at failure. This tensorial representation can take any direction in the continuum, but it must be expanded to at least a second order tensor for utility of an orthotropic material, or to a fourth order tensor to generalize damage through elimination of any material symmetry (Chaboche, 1995; Cauvin and Testa, 1999; Carol et al., 2001; Luccioni and Oller, 2003; Maimi et al, 2007).

There are two crucial considerations when modelling damage: the failure theory and ways to account for the damage. Typical failure criteria such as the maximum stress, the maximum strain, Hashin (1981), Tsai–Hill (1968), and Tsai–Wu (1971) are widely used because they are simple and easy to utilize (Christensen, 1997). In reviews by Daniel (2007) and Icardi (2007), wide variations in prediction by various theories were attributed to different methods of modelling the progressive failure process, the non-linear behavior of matrix-dominated laminates, the inclusion or exclusion of curing residual stresses in the analysis, and the utilized definition of ultimate failure. Camanho and Matthews (1999) achieved reasonable experimental/analytical correlation using Hashin's failure theory to predict damage progression and strength in bearing, net-tension, and shear-out modes.

To account for damage, progressive damage models of composite structures range from the simple material property degradation methods (MPDM) to more complex MPDM that combine CDM and fracture mechanics (Tay et al., 2005). Implementing a ply discount method whereby the entire set of stiffness properties of a ply is removed from consideration if the ply is deemed to have failed has been well established (Pal and Ray; 2002; Prusty, 2005; Maimi et al., 2007). Studies have also been performed attempting to generalize this procedure by replacing the constant degradation factor with a gradual stiffness reduction scheme (Reddy et al., 1995). Typical examples of MPDM utilize a 2D progressive damage model for laminates containing central holes subjected to in-plane tensile or compressive loading which are directly compared to experimental findings (Chang and Chang, 1991; Blackketter et al, 1993; Tan et al., 2005, Gorbatikh et al., 2007).

MPDM schemes are often implemented through user-defined subroutines (Chen et al., 1999; Xiao and Ishikawa, 2002; Goswami, 2005; McCarthy et al. 2005; Basu et al., 2007). Credited with being the first in this direction, Chang and Lessard (1991) performed similar work on damage tolerance of laminated composites in compression with a circular hole with similar results. These methods have been utilized for other conditions and have been used to develop a 3D analysis methodology based on the incorporating Hashin failure criteria into a similar logic (Evcil, 2008). By advancing to 3D, the error dropped down to 2.6% from as high as 30%. Others have continually built upon these accumulation CDM approaches giving them breadth across a wide variety of composite material, loading, and structural applications (Kwon and Liu, 1997; Icten and Karakuzu, 2002; Camanho et al., 2007; Liu and Zheng, 2008; Sosa et al., 2012; Su et al., 2015).

~~Additionally, material property degradation models and element failure method have been compared (Tay et al., 2005). While implementing a material property degradation method, as described by references above, it generalizes material and failure may be difficult to visualize. Implementing an element failure method attempts to address this by modification of nodal forces based on micromechanical failure criteria to model damage. Approaches such as these have shown promise when increases in scale are made from coupons all the way to structures; however, prediction beyond initial fiber or matrix failure is~~

~~questionable. This may be attributed to the oversimplification of the physical damage progression to a continuum model even though each constituent is accounted for independently.~~

1.2 Discrete Damage Modelling Background

In contrast, a DDM physically models the actual damage as it would physically occur~~s~~ through the load profile, typically as local failure of the constituents ~~and is considered by many to be~~ to be more consistent with the physical damage ~~observed in continuous fiber reinforced polymer composites~~. ~~As noted, a continuum approach relies on representing the damage as a change in material properties, whereas, observed damage is typically local failure of the constituents (matrix and/or fiber).~~ With ~~discrete~~ DDM approaches, constitutive properties do not physically change in a continuum sense, rather, ~~and~~ the degradation is a consequence of a local failure. ~~As such, d~~Damage is directly modelled as it would occur within a structure. In development of DDM approaches, knowledge *a priori* of the damage location is very helpful, though the result is they are generally computationally more expensive. ~~In addition, more time must also be spent in mesh creation. However, both modelling options have shown promise for modelling composite materials and the specifics of each method utilized are discussed below.~~

~~The Virtual Crack Closure Technique (VCCT) is a DDM that has been used with success for delamination growth in composite materials and structures. VCCT calculates the fracture energy at the crack tip by calculating the energy required to close the crack (Krueger, 2004). The work required to bring nodes together is used to calculate strain energy release rates. This technique is particularly useful for establishing or confirming critical strain energy release rates in either Mode I or II, G_{Ic} and G_{IIc}, respectively. The authors have used this for delamination growth modelling, but VCCT is a relatively mature procedure, the results are not presented.~~

~~Several techniques for discrete modelling exist such that crack development and path may be modelled. Originally, discrete models had discrete crack propagation and would be followed by a re-meshing with the new geometry. This cycle is repeated until ultimate failure has been reached based on one of several crack propagation criteria (Bouchard, et al., 2000). The discontinuity created by the crack can make re-meshing difficult and extended finite element modelling (XFEM) allows for a crack to propagate without having to re-mesh at each step (Areias and Belytschko, 2005).~~

The continual increase in computational availability has allowed for finer mesh refinement and paved the way for the use of cohesive elements for modelling laminated composites without an initial crack (Karayez et al., 2012). These zero thickness elements are useful with laminated composites because they may be placed between layers or fibers. A bi-linear traction-separation criterion is employed such that the element has a linear stiffness response until the maximum traction point is reached and damage is initiated. Then, the second portion of the bi-linear response estimates the damage evolution up to failure where separation occurs and the element is deleted. It is not necessary to know the bi-linear response as it may be developed iteratively using experimental/analytical correlation. While this method is computationally expensive due to extensive number of elements needed, this method has been shown to effectively model crack propagation.

3 Modelling Techniques

Several different modelling approaches were utilized ~~and each is outlined below~~to most accurately model the experimentation outlined in the testing companion paper (Nelson et al., 2017). It is important for the reader to note that all references to material testing and experimental results are from the work outlined in the companion paper. For each modelling approach, ~~a baseline linear elastic model was used and~~ the geometry was set up to match the intended coupon size (100 mm x 50 mm) of the 4-layer uni-directional fiberglass ~~established~~ used during material testing. ~~To determine if initial correlations were reasonable,~~ ~~2D~~Two-dimensional models ~~(Figure 4)~~ were generated with both ~~unflawed~~ non-wave and ~~IP~~ wave geometries (Figure 4), with quadrilateral, plane strain elements (CPS4), in Abaqus where each element was generated to be consistent with the nominal fiber tow width (1.0 mm). An unflawed case was tested for each method using the a fiber misalignment angle of 0° as verification of material properties and model setup. Porosity was also modelled with no fiber wave and material properties were degraded based on results from experimentation. The initial IP wave modelled had an amplitude (A) of 3.8 mm, a wavelength (λ) of 47.6 mm, and average off-axis fiber angle of 28.7°~~, though these were modified~~. Similarly, the initial OP wave modeled had an amplitude (*A*) of 2.9 mm, a wavelength (*λ*) of 22.8 mm, and average off-axis fiber angle of 19.4°. These variables were adjusted to match additional waves tested. Local coordinate systems were defined for the elements oriented to form the wave such that the fiber direction remained consistent through the wave~~, and the material properties were modelled to correctly match these properties~~. Since a symmetric wave was modelled, the number of elements was reduced using ~~A~~a symmetry boundary condition ~~was used~~ at the peak of the wave, as shown by the line of symmetry in Figure 4~~ allowing a reduction in number of elements~~ to reduce processing time. The elements edges along the line of symmetry were fixed vertically (1-direction), but were ~~allowed~~ not constrained~~ horizontally~~ otherwise. A ~~D~~displacement ~~and boundary conditions were~~ condition was applied at the ~~top~~bottom~~ and bottom, respectively,~~ to match the applied load during testing. ~~conditions discussed in the flaw evaluation and coupon testing companion to this paper (Nelson et al., 2017). and as such, full field calculations were set to match the testing data for load-displacement and stress-strain correlations.~~ Elastic material properties and damage progression determined in the coupon testing~~noted in testing~~ were utilized, as shown in Table 1 with a reduction based on Kerner's approach used for the 2% porosity case (Kerner, 1956). After solving, symmetry was applied to allow for calculation of the full–field average ~~calculation of~~ strain~~s~~ and stresses ~~allow~~ for comparison to the experimental testing. ~~The geometry shown in Figure 4 was utilized for all of the initial IP wave modelling efforts.~~

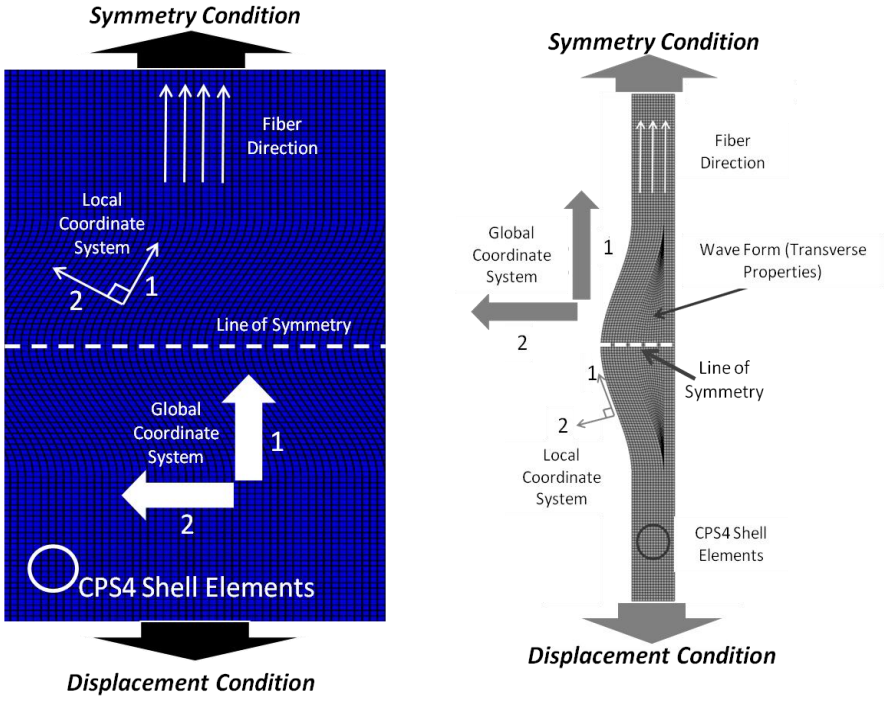

Figure 1: Representation of model and references used for IP (left) and OP (right) wave model.

Table 1: Empirical material properties utilized in Progressive Damage Analysis.

	Longitudinal Modulus (GPa)	Transverse Modulus (GPa)	Poisson's Ratio	Shear Modulus (GPa)
	E_1	E_2	v_{12}	G_{12}
Tension	40.6	16.3	0.27	16.8
Compression	38.4	14.4	0.28	14.4

Several assumptions were made to simplify this modelling effort. First, it was assumed that all fibers were parallel and uniform in the intended direction with reference to the width-wise edge, including through the ~~IP~~ wave. It was also assumed that all the fibers, for both the unflawed and ~~IP~~ wave geometries, were parallel and aligned through the thickness. These assumptions greatly simplified the modelling approach even though they were a possible source of the variation noted within the testing. In addition, perfect bonding between the layers was assumed. ~~Three distinct CDM and one DDM techniques were utilized to determine consistency, accuracy, and predictive capability compared to the testing results.~~

3.1 Hashin-based ~~Progessive~~Progressive Damage

~~First, t~~The Abaqus built-in a Progressive Damage and Failure for Fiber-Reinforced Materials (Abaqus~~Analysis User's Manual v6.12~~, 2012) that is intended to be used for elastic-brittle, anisotropic materials based on the Hashin failure criteria was utilized. In this case, the elastic response is defined as a linear elastic material with a plane stress orthotropic material stiffness matrix.

However, damage initiation must also be defined for the four included mechanisms: fiber tension, fiber compression, matrix tension, and matrix compression. ~~Once d~~Damage is initiated when one or more of these mechanisms reaches a value of 1.0 or larger based on the material strengths shown in Table 2: ~~in one or more of these mechanisms, elemental properties are degraded according to the defined damage evolution response~~:

Fiber tension ($\hat{\sigma}_{11} \geq 0$):
$$F_f^t = \left(\frac{\hat{\sigma}_{11}}{X^T}\right)^2 + \alpha\left(\frac{\hat{\tau}_{12}}{S^L}\right)^2 \quad (1)$$

Fiber compression ($\hat{\sigma}_{11} < 0$):
$$F_f^c = \left(\frac{\hat{\sigma}_{11}}{X^C}\right)^2 \quad (2)$$

Matrix tension ($\hat{\sigma}_{22} \geq 0$):
$$F_m^t = \left(\frac{\hat{\sigma}_{22}}{Y^T}\right)^2 + \left(\frac{\hat{\tau}_{12}}{S^L}\right)^2 \quad (3)$$

Matrix compression ($\hat{\sigma}_{22} < 0$):
$$F_m^c = \left(\frac{\hat{\sigma}_{22}}{2S^T}\right)^2 + \left[\left(\frac{Y^C}{2S^T}\right)^2 - 1\right]\frac{\hat{\sigma}_{22}}{Y^C} + \left(\frac{\hat{\tau}_{12}}{S^L}\right)^2 \quad (4)$$

where X^T is the longitudinal tensile strength, X^C is the longitudinal compressive strength, Y^T is the transverse tensile strength, Y^C is the transverse compressive strength, S^L is longitudinal shear strength, and S^T is transverse shear strength. In addition, ~~α is a~~ the shear stress contribution coefficient, α, was set to be equal to 1 as done by Hashin (1980). Next, elemental properties are degraded according to the defined damage evolution response given the energy release rates also in Table 2. Given that this method is built-in to Abaqus, the reader is refered to the Abaqus Analysis User's Manual section on Damage and Failure for fiber-reinforced composites (Abaqus, 2012).

Table 2: Damage initiation and evolution parameters utilized in Progressive Damage Analysis.

	Damage Initation (Strength) Parameters						*Damage Evolution (Energy Dissipation) Parameters*			
Property	Longitudinal Tensile (MPa)	Longitudinal Compressive (MPa)	Transverse Tensile (MPa)	Transverse Compressive (MPa)	Longitudinal Shear (MPa)	Transverse Shear (MPa)	Fiber Tension (kN/mm)	Fiber Compression (kN/mm)	Matrix Tension (kN/mm)	Matrix Compression (kN/mm)
Symbol	X^T	X^C	Y^T	Y^C	S^L	S^T	G^c_{ft}	G^c_{fc}	G^c_{mt}	G^c_{mc}
Value	990	582	60	35	112	124	16	16.9	39.9	45.1

3.2 User-defined Subroutine

Next, a user-defined subroutine was employed with a combined maximum stress/strain user specified failure criteria where the standard input file builds and meshes the model, while the user subroutine checks for damage at each step. If damage is detected, the material properties were adjusted or the loop is stopped if ultimate failure has occurred. If damage is detected, but not ultimate failure, the material properties are degraded depending on the type of failure as outlined in Table 3 based on the three independent failure types: matrix cracking, fiber-matrix damage, and fiber failure. Based on the procedural logic from

Chang and Chang (1987), an Abaqus code was written with a Fortran subroutine acting as the inner loop following the decision tree shown in Figure 5 (Chang and Lessard, 1991).

Table 3: Progressive Damage Analysis degradation for User Defined Criteria

Material Failure Type	Elastic Property Adjustments for Each Failure Type				Notes
No Failure	E_x	E_y	v_{xy}	G_{xy}	Full properties.
Matrix Cracking Damage	E_x	0	0	G_{xy}	Used in tensile and compressive cases.
Fiber-Matrix Damage	E_x	E_y	0	0	Fiber compresses & matrix cracks; used in compression only.
Fiber Failure	0	0	0	0	Fiber buckles or breaks; all properties drop to zero.
Combined Matrix Cracking & Fiber-Matrix Damage	E_x	0	0	0	Fiber is still intact and able to carry some longitudinal load.
Combined Matrix Cracking Damage & Fiber Failure	0	0	0	0	All properties drop to zero.
Combined Fiber-Matrix Damage & Fiber Failure	0	0	0	0	
All Combined Failure Modes	0	0	0	0	

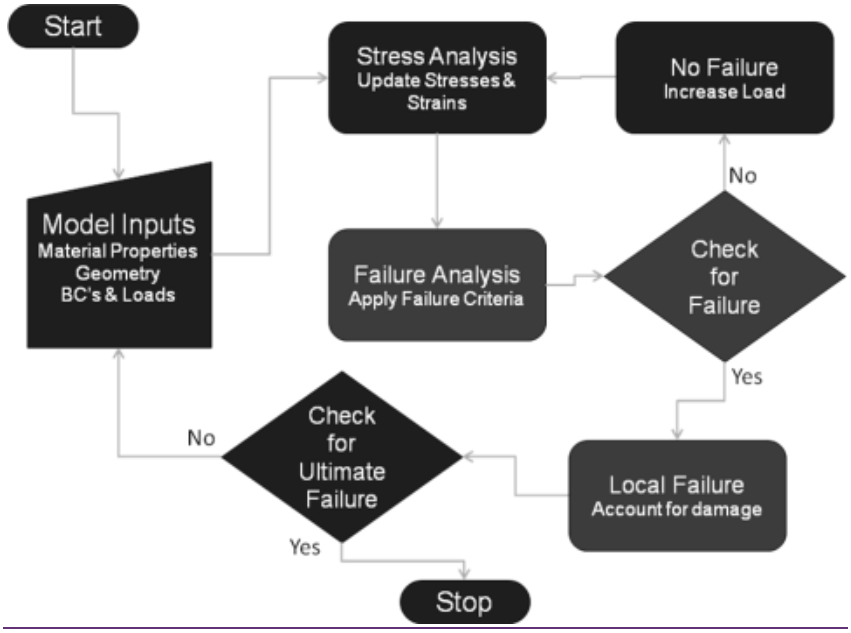

Figure 2: Decision tree for progressive damage modelling utilized in this modelling.

To determine the failure values, ~~user-defined failure criteria integrating~~ both maximum stress and strain criteria were implemented into the subroutine utilizing the damage initiation values in Table 2~~Table 2~~ and a strain at failure of 2.6%. A modified maximum stress failure criterion was implemented with the inclusion of a maximum strain criteria to accurately model ultimate ~~fiber~~ matrix failure. As such, matrix cracking damage was estimated by:

$$\left(\frac{\sigma_{22}}{Y_T}\right)^2 + \left(\frac{\tau_{12}}{S_T}\right)^2 = 1 \quad (5\text{~~10~~})$$

where σ_{22} and Y_T are transverse stress and transverse strength, respectively, and τ_{12} and S_T are shear stress and strength, respectively. It must be noted that this same equation was utilized for both tensile and compressive cases, and the associated material properties ~~are~~ were changed for each case. While the fiber-matrix compression damage case appeared to be necessary only in compression loading cases, with the given geometries these failure criteria were utilized in both tensile and compressive cases:

$$\frac{\sigma_{11,C}}{Y_C} + \frac{\tau_{12}}{S_T} = 1 \quad (6\text{~~11~~})$$

where $\sigma_{11,C}$ and Y_C are fiber compressive stress and strength, respectively. Finally, two different equations were manually utilized depending on whether fiber failure is in tension or compression, respectively:

$$\frac{\varepsilon_{11,T}}{\bar{\varepsilon}_T} = 1 \quad (7\text{~~12~~})$$

$$\frac{\sigma_{22,C}}{X_C} = 1 \quad (8\text{~~13~~})$$

where $\varepsilon_{11,\mathrm{T}}$ and $\bar{\varepsilon}_{11,\mathrm{T}}$ were calculated for ultimate tensile strain and compressive stress, respectively. Utilization of the maximum strain criterion in tension was based on the consistency of strain at failure of these materials as determined in the testing. Integration of this criterion was a fundamental motivation in utilizing this user-defined technique.

A standard Abaqus code was written for an elastic material with 3 dependencies to match the independent failure types before calling out a **USER DEFINED FIELD* to call the subroutine into use. The subroutine itself was rewritten from the FORTRAN example found in the Abaqus Example Problem 1.1.14 and the reader is referred to this reference directly for the code specifics (Abaqus, 2012). First, the subroutine established the specific material parameters taken from the experimentation as noted in Tables 1 and 2 above. Next, the failure variables were initialized and the stresses were retrieved from the previous increment. Next, the crucial portion of the code was reached where the stresses were used to check for failure in each of the cases, or each dependent variable is determined. An *IF* loop was utilized for each of the Equations 5-8 noted, with 7 and 8 being manually swapped out for tension and compression, respectively. For example, considering the matrix damage portion, the loop first determined that if the matrix cracking damage variable was less than one (Table 3), the loop then recalculated with the updated stresses before updating the appropriate state variable. No calculation was necessary if the value was one because failure already occurred. Finally, the state variables were used to update the field variables which were then passed back to the standard code, and the loop was ended.

Thus, at each increment the subroutine ran through the~~se~~ failure criteria equations that ~~utilize~~ analyze the stress and strain data of that increment. Resulting values of these equations range from zero (0) to one (1) with failure occurring when the value was equal to one (1). As the failure indices were calculated to be one (1), failure ~~has~~ occurred in that element and the material

properties were adjusted based on the failure type as noted in Table 3. For example, if a matrix failure occurred, the failure indices included in the user subroutine calculated that Failure Value #1 became equal to one (1). As a result, the elastic properties for that element only include E_x and G_{xy} as these are fiber dominated. The loop continued with the degraded properties until fiber failure or a combination of failures occurred resulting in no material properties for that element.

3.3 Non-linear Shear Model

Based on the shear between the fiber tows in the wavy area, it was deemed that a non-linear constitutive law needed to be developed for the bulk material using a user defined material subroutine (UMAT) in Abaqus (2012). As observed in the experimental testing and indicated by VanPaepegem et al. (2006), unrecoverable damage or plasticity occurs through the shear response. A method to degrade the shear material properties based on the shear response generalizing this damage and plasticity was implemented. Based on the change in shear modulus during this degradation, 8 points were identified where changes in secant modulus were noted as identified in Figure 3~~Figure 3~~. ~~Using t~~The tabulated shear stress-strain relationships ~~(Figure 5, left),~~ were used to determine the shear stress and tangential modulus ~~were calculated~~ by the subroutine once the stress for the increment was calculated:

```
SUBROUTINE UMAT_SHEAR_STIF(SHEAR,GAMMA,TAU,GG12,G12,STRESS3)
      IMPLICIT REAL*8(A-H,O-Z)
      DIMENSION GAMMA(*),TAU(*),GG12(*)
      IF   (SHEAR.LT.GAMMA(1)) THEN
           G12=GG12(1)
           STRESS3=G12*SHEAR
      ELSEIF(SHEAR.LT.GAMMA(2)) THEN
           G12=GG12(2)
           STRESS3=TAU(1)+G12*(SHEAR-GAMMA(1))
      ELSEIF(SHEAR.LT.GAMMA(3)) THEN
      ⋮
{SIMILAR ELSEIF STATEMENTS CONTINUE FOR THE NEXT 4 STRESS LEVELS}
      ⋮
      ELSE
           G12=GG12(8)
           STRESS3=TAU(8)+G12*(SHEAR-GAMMA(8))
      ENDIF
      RETURN
      END
```

~~-~~Once the shear stress and modulus were determined, the~~and~~ update~~s~~ were returned~~d~~ into the material card of the model. ~~Shear stress-strain from the actual materials used for these tests data was then utilized in the UMAT and a zero stiffness condition was approximated to ensure model convergence.~~

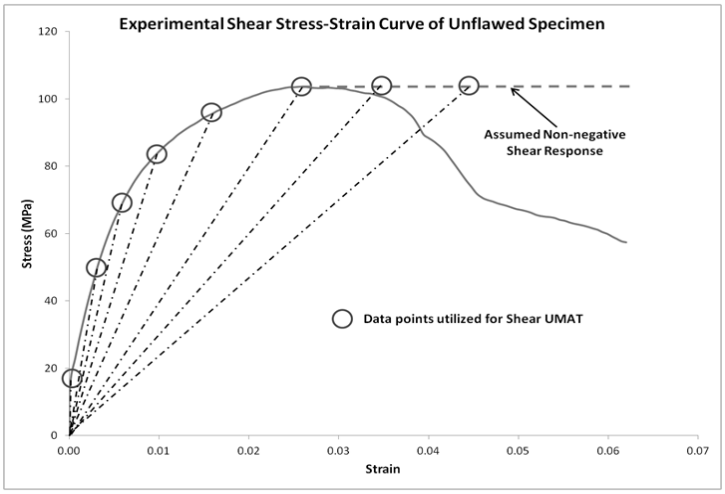

Figure 3: Keypoints from empirical shear stress-strain relationship used in the non-linear shear UMAT.

3.4 Cohesive Zone Model

To model damage progression discretely, cohesive elements are typically utilized based on a cohesive law relating traction to separation across the interface (Karayev et al., 2012; Lemanski et al., 2013). Zero thickness elements with specific bi-linear traction-separation criteria (Figure 5, right) were placed between the fiber tows. While following ~~previous~~ convention ~~was~~ to utilize cohesive elements only in specific areas, ~~predefining the crack path,~~ computational availability has made it conceivable to place cohesive elements between all fiber tows throughout the model. Thus, damage and crack progression ~~may~~ was able to occur between any fibers ~~virtually anywhere in the model~~ ~~where the~~based on the stress state. ~~indicates rather than where the user has placed these elements.~~

A bi-linear traction-separation criterion was ~~used as shown in~~(Figure 4~~Figure 4 Figure 5~~) where the initial stiffness, K, of the cohesive element is linear up to the damage initiation point at critical separation, Δ_c. From this point to the failure separation, Δ_{fail}, the slope estimates the damage evolution of each the cohesive element up to failure. The traction-separation criterion is met for a specific cohesive element and a separation occurs resulting in crack propagation and element deletion. ~~As such, damage progression can be modelled discretely. Based on the inexact ability to determine these parameters, they must be adjusted in an iterative approach resulting in multiple model runs to establish reasonable analytical/experimental correlation. Such parametric studies were performed to ensure that these cohesive properties do not impact the stiffness and response of the surrounding material in ways other than those intended.~~ A standard material specification was used and parametric studies were performed to determine the stiffness and maximum traction properties of the cohesive elements (Figure 5~~Figure 5~~). Initial model analyses were performed to determine the cohesive element stiffness, K_{eff}. Analyses were performed at various stiffness values to determine the convergence value of 5E6 N/mm by performing several model runs to determine convergence point (Figure 5~~Figure 5~~a). Similarly, the effects of T_{1max} were determined by analyzing several different values and it was determined that failure behavior was not dependent on T_{1max} (Figure 5~~Figure 5~~b). However, when a similar test was analyzed for T_{2max} it

was quickly apparent that the failure was sensitive to Mode II shear damage (Figure 5~~Figure 5~~c). The peak tractions (T_{1max} = T_{2max} = 100 MPa) were then used in an initial run as shown in Figure 5~~Figure 5~~d to confirm these values and ensure that the cohesive elements were not influencing initial stiffness correlations. A B-K mixed mode criterion was utilized where G_{Ic} and G_{IIc} were 806 J/m^2 and 1524 J/m^2, respectively, as found experimentally (Benzeggagh and Kenane, 1996).

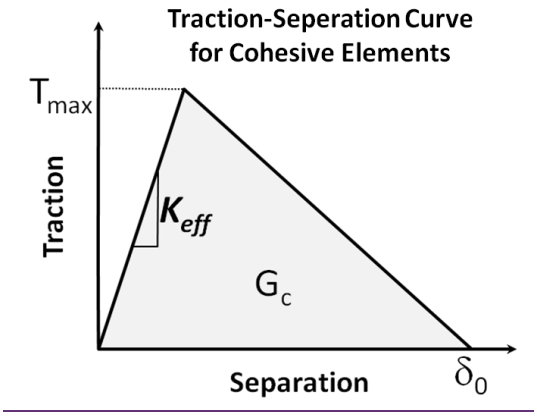

Figure 4: Representation of bi-linear traction-separation response for a cohesive element.

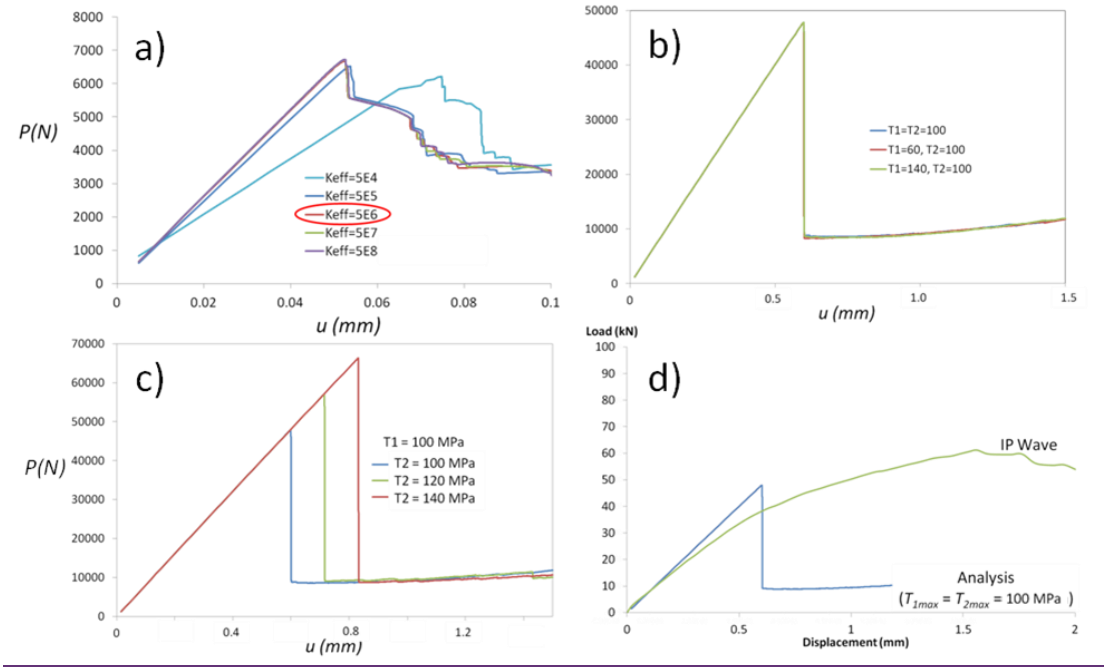

Figure 5: Results of parametric studies to find cohesive element: a) effective stiffness, K_{eff}; b) peak Mode I traction, T_{1max}; c) peak Mode II traction, T_{2max}; and, d) confirmation of peak tractions.

3.5 Combined Non-linear Shear and Cohesive Zone Model

~~Based on the results of the individual methods noted above, a~~The non-linear shear CDM ~~was combined with~~ and the~~a~~ DDM using cohesive elements were combined due to their poor overall performance individually. As discussed below, in both cases, the models seemed to capture portions damage progression, while each lacked the exact progression observed in the testing. In this case, the methods described in Sections 3.3 and 3.4 above, were combined by adding the non-linear shear routine to the cohesive zone model with the same material properties and parameters utilized from the material testing and parametric studies performed. ~~It was believed that by combining them, the interaction of the two model types would result in a consistent, accurate, and predictive analytical tool.~~

2 Model Validation ~~& Tuning Systematic Approach~~ Methodology

A systematic approach, as shown in Figure 2, was employed to validated and compare different modelling methods ~~discussed (Figure 2)~~. A qualitative/quantitative approach was utilized similar to that utilized by Lemanski et al. (2013), though strains at peak stress were also considered. Acceptable models correlated well both qualitatively, by matching failure location and shape, and quantitatively, by matching initial stiffness and peak stress at failure strain. First, a qualitative assessment was performed and correlation was deemed acceptable if strain accumulation and damage progression visually matched the testing results.

Using digital image correlation results from the material testing allowed for quick analysis of several key factors including an energy comparison. An energy comparison ensured that the energy was conserved between the strain energy available and energy dissipated. A visual ~~C~~comparison of the unrecoverable energy, or area under the curves, was deemed sufficient as models that do not conserve energy were evident and were not considered acceptable.

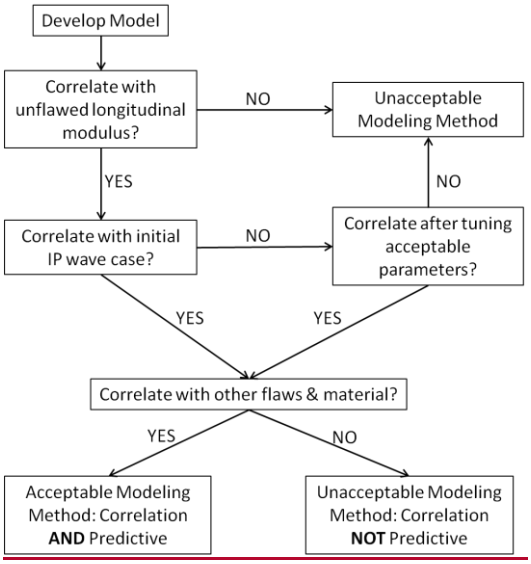

Figure 6: Systematic flow of approach to determine acceptability of each model.

If the qualitative criteria were met, a quantitative assessment was performed. First, the strain at peak stress was compared and deemed acceptable if it was within ±10% of testing results. If acceptable, peak stress was compared and deemed acceptable if it was within ±10% of testing results. The value of 10% was chosen for both of these parameters as it was the smallest range of all of the experimental variability as shown in ~~These areas of quantitative acceptability are shown in~~ Figure 3. While these acceptance criteria were beyond the variability noted in the testing, if these criteria were outside ±10%, but within ±20%, correlation was considered moderate and model modification was performed. It is important to note that this consideration was only made for correlation with other flaws after acceptable correlation had been achieved for the initial IP wave case. As such, models were considered predictive if correlation was achieved with these other cases utilizing the same input parameters as the initial IP wave case.

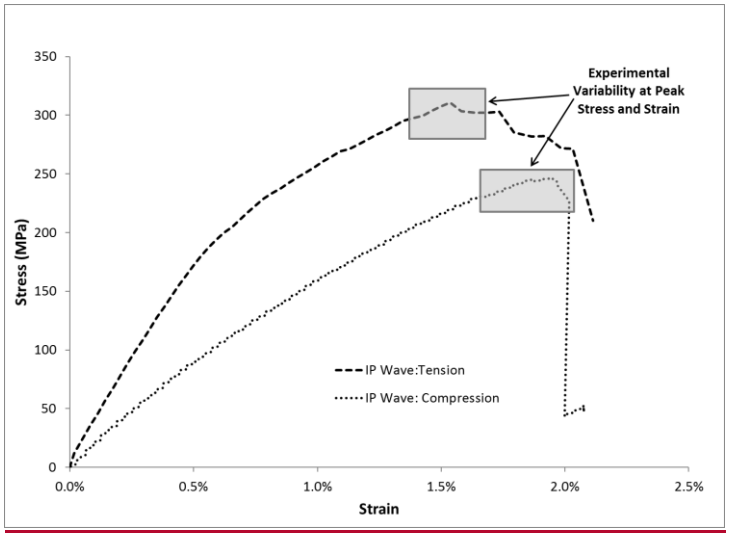

Figure 7: Tension and compression response of IP Wave 1 utilized for baseline correlations with associated experimental variability.

As shown in Figure 2, if correlation was not achieved by a model at any point during the systematic increase in flaw complexity, the model was deemed unacceptable and no additional flaw geometries were tested. The increase in flaw complexity in each case ~~went~~progressed from unflawed controls to porosity to the IP wave baseline case (Figure 1~~Figure 1~~, left) to the initial OP wave case (Figure 1~~Figure 1~~, right), and then to other IP and OP geometries. Acceptable models were able to accurately and consistently predict each of these cases, and with this consistent systematic approach, the different techniques were ~~able to be~~ compared ~~easily~~.

The analytical models presented above were created, run, and correlated to responses outlined in the testing effort and modified to improve correlation if found to be outside the ±10% indicated above. As shown in Table 4~~4~~, the specific input parameters for each model are shown as well as the parameters that were acceptable to tune within the ranges of the variability seen during experimentation. Acceptable tuning parameters within the variability noted from the experimental results was performed only to assist with convergence, and the effects on the model were directly tracked. It is critical to note that no results included were from modifications made to any elastic properties shown in Table 1~~Table 1~~.

Table 4: Input parameters and acceptable parameters for modification with range of acceptable modification.

MODEL TYPE	*MODEL*	*INPUT PARAMETERS*	*PARAMETERS AND RANGE OF ACCEPTABLE MODIFICATION*
CDM	Linear Elastic	ELASTIC PROPERTIES	NONE
	Linear Elastic w/ Hashin Failure Criteria	ELASTIC PROPERTIES & DAMAGE INITIATION & EVOLUTION	DAMAGE INITIATION & EVOLUTION (± 10% OF VALUES TABLE 2)
	Subroutine w/ User-defined Damage Criteria	ELASTIC PROPERTIES, DAMAGE INITIATION, & FAILURE CRITERIA	DAMAGE INITIATION (± 10% OF VALUES TABLE 2)
	Non-Linear Shear	ELASTIC PROPERITES & STRESS-STRAIN FROM UNFLAWED SHEAR RESPONSE	ADJUSTMENT OF POINTS FROM SHEAR STRESS-STRAIN RESPONSE (FIGURE 3)
DDM	Cohesive Elements between Tows	ELASTIC PROPERTIES & COHESIVE TRACTION-SEPARATION	COHESIVE TRACTION-SEPARATION (PARAMETRICALLY DETERMINED IN FIGURE 5)
Combined	Non-Linear Shear w/ Cohesive Elements between Tows	ELASTIC PROPERTIES, STRESS-STRAIN FROM UNFLAWED SHEAR RESPONSE, & COHESIVE TRACTION-SEPARATION	ADJUSTMENT OF POINTS FROM SHEAR STRESS-STRAIN RESPONSE (FIGURE 3) & COHESIVE TRACTION-SEPARATION (PARAMETRICALLY DETERMINED IN FIGURE 5)

4 Results & Discussion

The final results from each model following the validation methodology are summarized in Table 5~~Table 5~~. These results are discussed through the progression of increasing complexity (unflawed, porosity, IP wave, OP wave, and additional waves, respectively) for each model. Each model was scored based on the acceptance criteria with acceptable correlation (A), moderate correlation (M), and unacceptable correlation (U). There were several cases where experimental results were not yet available due to complexity of testing (R). Also, once a method was deemed unacceptable no additional models were run through the increasing complexity (NR). It should be noted that a modulus check (MC) on the unflawed specimen confirmed modulus correlation.

Table 5: Summary of results of each model for acceptability.

		UNFLAWED		POROSITY		IP WAVE		OP WAVE		ADDITIONAL WAVES	
MODEL TYPE	MODEL	Tension	Comp	Tension	Comp	Tension	Comp	Tension	Comp	Tension	Comp
CDM	Linear Elastic	MC	MC	NR	NR	NR	NR	NR	NR	NR	NR
	Linear Elastic w/ Hashin Failure Criteria	MC	MC	A	M	A	M	M	R	A,U	NR
	Subroutine w/ User-defined Damage Criteria	MC	MC	NR	NR	U	U	NR	NR	NR	NR
	Non-Linear Shear	MC	MC	NR	NR	U	U	NR	NR	NR	NR
DDM	Cohesive Elements between Tows	MC	MC	NR	NR	U	U	NR	NR	NR	NR
Combined	Non-Linear Shear w/ Cohesive Elements between Tows	MC	MC	NR	NR	A	A	A	R	A,U	R

KEY:
A = ACCEPTABLE CORRELATION (visual correlation and within 10% of Strain at Peak Stress & within 10% of Peak Stress)
M = MODERATE CORRELATION (visual correlation but marginal quantitative acceptance criteria)
U = UNACCEPTABLE CORRELATION (unacceptable visual and/or quantitative correlation)
R = MODEL RUN BUT NOT CORRELATED (insufficient test data available)
NR = MODEL NOT RUN (due to unacceptable initial case or acceptable overall method)
MC = INITIAL MODULUS CHECK (stiffness of model within 5% of test)

4.1 ~~Qualitative Damage Progression Comparison~~Unflawed and Porosity Correlations

For each modelling technique, a qualitative analysis, and then a quantitative analysis, was performed. The impetus of this was to ensure that the progressive damage models were consistent with the observed progressive damage in tests. The preliminary step for each model case was ensure the unflawed material response matched experimental results. Given the simplicity of the check, only a qualitative comparison of the initial modulus was made. In all cases, correlation was found to be within 5% as shown for a representative case in Figure 8~~Figure 8~~, left. A similar result is noted for the 2% porosity case correlation for the linear elastic with Hashin failure criteria (Figure 8~~Figure 8~~, right). Given the good correlation between this method and the ease-of-use with the Kerner method of property reduction, no other modelling methods were examined for porosity. In short, this method was seen to meet the goal of an acceptable method of modelling this type of manufacturing defect found in wind turbine blades. Results in compression were similar for both cases, but were only considered moderate for the porosity case due to large variation noted in the experimentation.

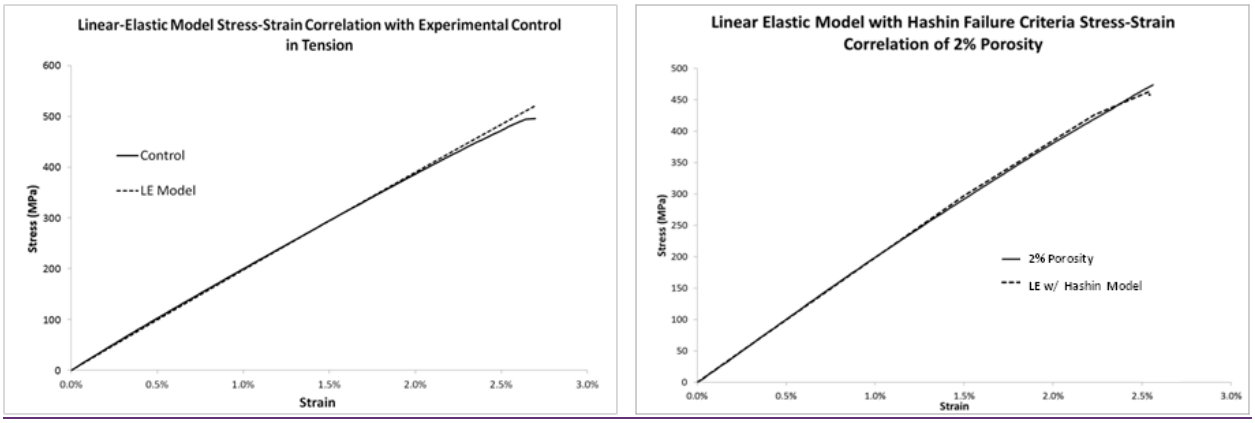

Figure 8: Correlation of analytical and experimental results for the unflawed (left) and porosity (right) cases.

4.2 Initial IP Wave Correlations

~~For each modelling technique~~technique, ~~a qualitative analysis, and then a quantitative analysis, was performed. The impetus of this was to ensure that the progressive damage models were consistent with the observed progressive damage in tests. Images were analyzed and qualitative comparisons were made through the damage progression as exemplified in Figure 6.~~Assessment of the correlations from modelling the initial IP wave case resulted acceptance of the Hashin and combined methods, but rejection of other methods (Table 5~~Table 5~~) A representative case comparing the as-tested IP wave with the combined model results at similar displacements is shown below in . The qualitative comparison was performed by comparing the experimental images, taken from the data set shown with experimental stress-strain curve, at displacements of 0.5 mm and 2.0 mm with the model images generated at similar displacements. It is important to note by identifying these displacements on the stress-strain curve, these snapshots indicate a similar progression. ~~while~~ The reader is reminded that for the experimentation full-field averages were used for strains and a comparable approach was used for modelled strain allowing for direct energy comparison~~energy dissipation to be compared~~. In ~~Figure 6~~ (left), it may be seen that failure occurred first at the edges where fibers were discontinuous at low loading which matches the degradation noted in both stress-strain curve. As ~~the~~ load increased, damage accumulation may be noted in the fiber misalignment section with shear failure occurring in the matrix as the fibers straightened due to tensile elongation (~~Figure 6~~, right). As may be expected, the failure areas are cleaner and less complex for the models due to uniformity and symmetry of the modelled specimen. ~~Notably~~For this case, the qualitative correlation was quite consistent through the initial, low-load portion of each analysis where shear load increased significantly through the wavy section for all the modelling techniques.

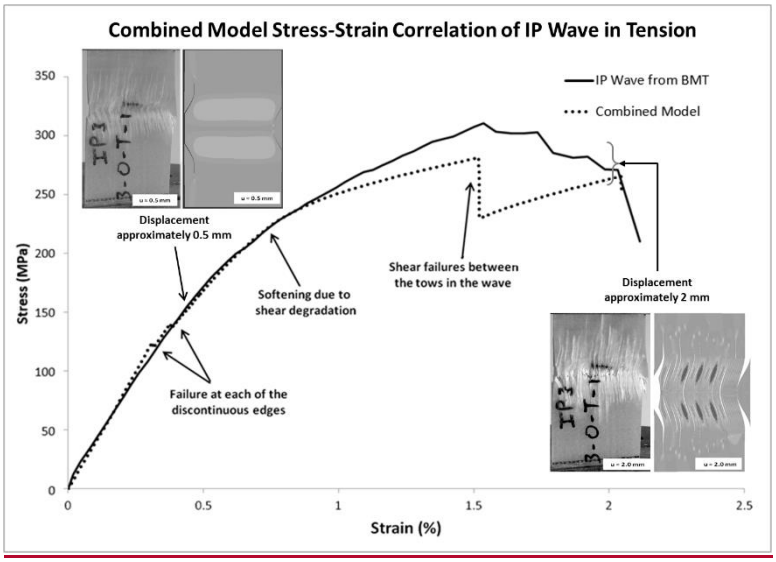

Figure 9: Comparison of damage at displacements of approximately 0.5 mm and 2 mm between experimental (above) and analytical (below) showing onset-to-final damage left-to-right, respectively, with points and damage progression identified on resulting stress-strain curve.

Figure 86: Comparison of damage at displacements of approximately 0.5 mm and 2 mm between experimental (above) and analytical (below) showing onset-to-final damage left-to-right, respectively, with points and damage progression identified on resulting stress-strain curve.

4.2 Quantitative Material Response Comparison

For each technique, stress-strain relationships were generated using the same method of far-field strain utilized during experimentation (Figure 7). Where response appeared to be similar from the qualitative analysis, the differences in the responses from modelling techniques is clearly quantified. To summarize the comparisons, Table 4 outlines the graded results of each model technique while noting both the input parameters and the parameters acceptable for tuning. Following the systematic approach, a modulus check (MC) was performed first for all cases. Next, a CDM approach where material properties were degraded based on amount of included air was performed for porosity and acceptable correlation (A) was achieved in tension. However, while the results appeared reasonable in compression, experimental data was not sufficient to perform correlation (R). In order to consider fiber waviness, each model was checked for the same initial IP wave case before moving on to consider other waves and/or materials if acceptable correlation was found. Finally, no addition cases were run for a model if correlation for this initial case was found to be unacceptable (U). This was found to be the case for the user-defined failure criteria, non-linear shear, and cohesive element models which showed poor correlation. However, the Hashin failure criteria model and the combined model were found to have good correlation, resulting in further testing. The results of each method are discussed below.

The resulting stress-strain curves from each model are shown in Figure 10Figure 10. While the Hashin failure criteria successfully met the acceptance criteria, it did not exactly match the experimental material response particularly from 0.5-1.5% strain in tension (Figure 10Figure 10). In addition, correlation was only moderately acceptable in compression due to under-prediction of softening and over-prediction of final failure noted in Figure 10Figure 10, right.

A linear elastic model was modified to include the Hashin failure criteria built into. First, a model was created and utilized for porosity before the initial IP wave case was run. For porosity, the criteria for acceptable and marginal correlations were achieved for tension and compression, respectively. Given these results and the predictive ability when varied for different amounts of porosity, the approach was deemed acceptable and further investigation was not performed. For the initial IP wave case, regions of acceptability were noted and was improved when the acceptable parameters (damage initiation, evolution, and stabilization) were adjusted (Figure 7). Once the initial model was tuned, additional wave and material cases were run as indicated in Table 4 and found to be predictive in all cases indicating the promise of this method.

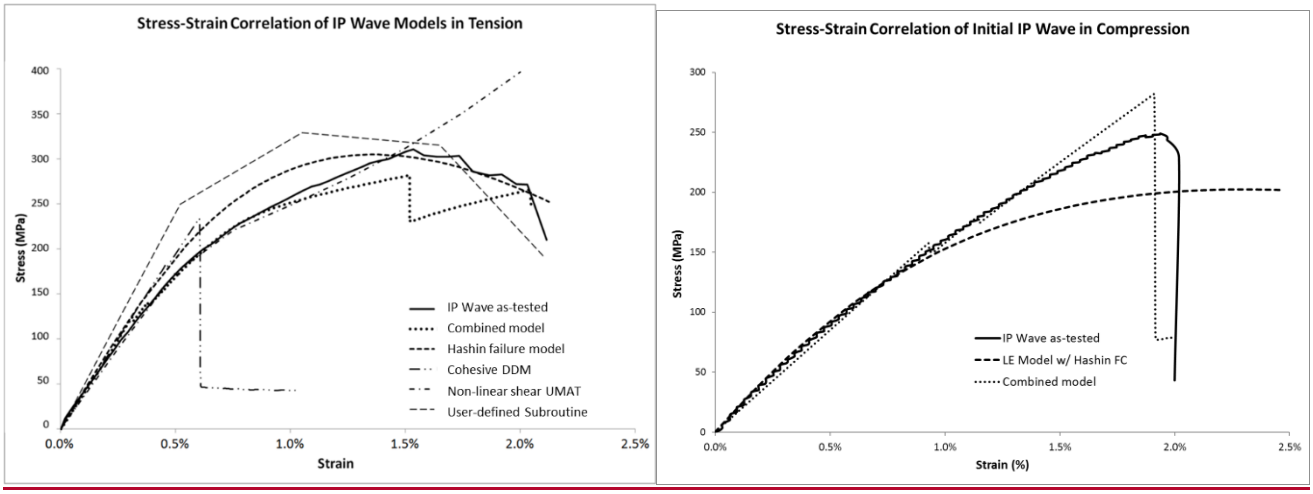

Figure 10: Resulting initial IP Wave tension (left) and compression (right) stress-strain curves of each model compared to experimental results.

~~While the Hashin failure criteria successfully met the acceptance criteria, it did not exactly match the experimental material response particularly from 0.5-1.5% strain (Figure 9Figure 7).~~ In an unsuccessful attempt ~~order~~ to offer the user more control to improve the modelling of the material response, the subroutine with user-defined failure criteria was used. As seen in Figure 10~~Figure 10~~, the results in tension did not match the acceptance criteria even ~~A~~after ~~significant tuning~~modification of the material property degradation scheme~~. , sufficient correlation was not achieved and the response showed a greater difference than the Hashin failure criteria in the area of interest.~~ As such, this approach was deemed unacceptable, as noted in Table 5~~Table 5~~~~Table 4~~ and no further attempts at correlation were attempted.

~~Both a CDM using a non-linear shear response and a DDM using cohesive elements, respectively, were attempted independently.~~ While neither the non-linear shear subroutine nor using cohesive elements ~~case~~ was able to accurately model the experimentally observed response, ~~each showed an~~ areas of promise were identified in tension. The non-linear shear response matched the experimental response up to failure more accurately than any other model (Figure 10~~Figure 10~~~~Figure 7~~) up to approximately 1.4% strain. At this point, the model showed the wavy fibers had essentially straightened resulting in the increased stiffness indicated. Given this was not seen experimentally, the approach was deemed unsuccessful. Similarly, when cohesive elements were placed between the fiber tows, matrix damage was modelled, though the peak stress and strain were both under-predicted. Since neither ~~was able to~~ modelled the experimental damage progression, neither was used independently for additional cases (Table 5~~Table 5~~~~Table 4~~).

However, ~~B~~based on the individual responses of these two techniques, a model was created placing cohesive elements between the fibers of the non-linear shear ~~UMAT~~ subroutine model. When used to model the initial IP wave case the response correlated to the experimental data. Specifically, the combined model curve and experimental IP wave curve had similar responses up to 0.5% strain as shown in Figure 10~~Figure 10~~~~Figure 7~~. Above this point the model under-predicted the peak stress, which was attributed to the uniformity of the model which was based on the average fiber misalignment angle. As such, the material

failed through-the-thickness where all fibers were perfectly aligned, but the experimental specimens were not as consistent and some layers had a smaller fiber misalignment angle which increased the load carrying capability. Regardless, the combined model was within the acceptable range and matched strain at failure where the cohesive failures caused the sudden drop in load-carrying capability. Based on this result, and the moderate correlation in compression (Figure 10~~Figure 10~~), additional correlations were attempted resulting in the best combination of accuracy, consistency, and predictive capability of all the modelling techniques tested (Table 5~~Table 5~~~~Table 4~~).

4.3 Initial OP Wave Correlations

~~HASHIN…~~ Both the Hashin and combined models ~~The model was also~~were run for the compression case ~~(as shown in Figure 68, right) and while the compression case seemed reasonable, there are no data for comparison, and so no correlation was made; however, the model is ready when future data become available.~~

~~COMBINED…As above, quantitative c~~Correlation was performed by comparing the full-field stress-strain data from the ~~BMT~~experimental to the model results. As noted, no changes were made to the input model parameters other than the change in model geometry. ~~The~~Both models captured initial stiffness quite well up to approximately 1.5% strain where it is clearly evident that the Hashin model was divergent resulting in only moderately acceptable correlation. For the combined model ~~at which point~~ the first cohesive failures were noted at this strain though, ~~which aligned with the transition from Figure 108a-b.~~ l~~L~~oad redistribution occurred and the model predicted the additional load-carrying ~~seen through Figure 108c~~ before additional cohesive failures ~~and manual truncation occurred~~. While the correlation was not perfect, it met the acceptance criteria. ~~matched fairly well. Tuning may be applicable as future work with additional testing and especially with improved understanding of response when this flaw is embedded into a substructure or structure.~~

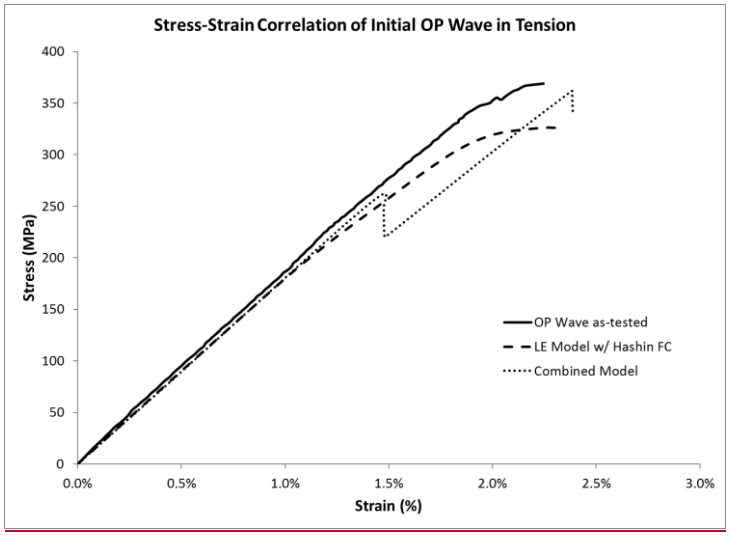

Figure 11: Resulting initial OP Wave stress-strain curves of each model compared to experimental results.

In summary, even though each model appeared to have different strengths, only the Hashin failure criteria and combined modelling techniques met the acceptable limits of the systematic approach employed. In both cases, this was true not only for the initial IP wave case, but also for additional wave and material cases (Table 6Table 4). After initial tuning of the damage parameters, the Hashin failure criteria model showed acceptable correlation in tension and moderate correlation in compression, while the combined model was acceptable for both. In tension, the combined model more accurately predicted both the initial stress-strain response and damage, even though the computational time was five times longer. when considering all cases, the combined approach was the found to be most the accurate, consistent, and predictive.

4.4 Additional Wave Correlations

HASHIN…To match the experimental work, additional waves were modelled at 16° and 48° with no other changes made to any input parameters to assess the predictive capability of both the Hashin and combined approaches. For the Hashin approach, While the initial case above, over-predicted the load-carrying capacity after initially matching the stiffness, it very closely matched the appropriate stress at the ultimate failure strain. Neither of these bounding cases matched this result, but they both showed similar variations (Figure 70). The 16° case matched the initial stiffness and, similar to the initial 29° case, over-predicted the load-carrying capacity before ultimately under-predicting the ultimate failure stress by just over 10%. The 48° case also matched the initial stiffness and over-predicted the load-carrying capacity. However, instead of being conservative this case also over-predicted the ultimate failure stress by almost 40%. Given only moderate results in compression above, the compression case was not run.…

COMBINED….For the combined case Similar initial stiffness results were noted in both the 16° and the 48° IP wave cases. Instead of an over-prediction of the softening, a slight under-prediction was noted in the 16° case, while the 48° case appeared to match the overall softening quite well. As seen in Figure 1212Figure 113, the 16° case had an initial damage kink before softening began resulting in an under-prediction of peak stress of approximately 4.8%. The model then matched, within the same range, the continued load-carrying capacity up to truncation at failure of 2.05% strain. The 48° case told a different story and saw the best correlation of any model case in this entire study through softening. However, shortly after the kinks associated with the delaminateding in theof discontinuous fiber sections, a significant number of cohesive elements failed resulting in a significant drop in load-carrying capacity, but not in final failure. As such the peak stress was noted at approximately 1% strain and was found to be almost 20% below the peak stress noted in the model at 1.7% strainmeaning correlation was unacceptable. After this peak, however, a slight increase in load-carrying capacity was noted up to truncation at failure of 2.4% strain. As noted abovBased on this result e only the 16° combined model yieldedwas correlated useful results in compression. The results were very similar to the initial case shown in Figure 1212Figure 104 where stiffness was initially slightly low for the model and was again attributed to variation in the BMT coupons tested. In this case, the only one initial kink was noted and a stiffness change was associated with it. Unlike the initial case, the second kink occurred just

before the peak stress which was over-predicted by approximately 5.1% with a predicted strain of 1.6% instead of the almost 1.8% ~~from the BMT~~observed experimentally.

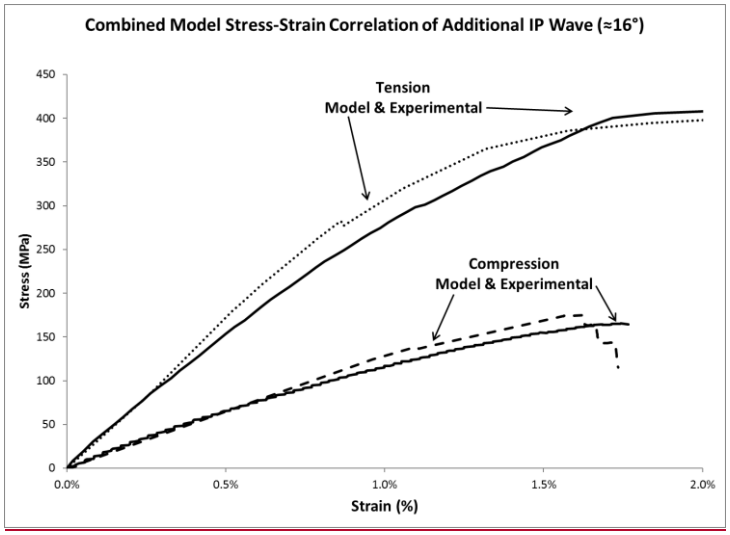

Figure 12

5 Conclusions & Future Work

In summary, even though each model appeared to have different strengths, only the Hashin failure criteria and combined modelling techniques met the acceptable limits of the systematic approach employed. In both cases, this was true not only for the initial IP wave case, but also for additional wave and material cases (Table 5~~Table 5~~). After initial tuning of the damage parameters, the Hashin failure criteria model showed acceptable correlation in tension and moderate correlation in compression, while the combined model was acceptable for both. In tension, the combined model more accurately predicted both the initial stress-strain response and damage, even though the computational time was five times longer. when considering all cases, the combined approach was the found to be most the accurate, consistent, and predictive.

To assess and predict the effects of manufacturing defects common to composite wind turbine blades, a comparison of several different damage progression models was performed resulting in several conclusions. Findings indicate that when material properties generated from unflawed material testing were used, all models were able to predict initial laminate stiffness when flaw geometries are discretely modelled. Models were run and a systematic approach was followed to assess the results compared to experimental results of flawed specimen. Specifically, the CDM using Hashin failure criteria was found to be accurate, consistent, and predictive particularly in tension for all wave and material cases once the damage properties were found. To account for the variations noted and improve the accuracy, a user-defined failure criteria was run, but results were not within the acceptable limits. Next, non-linear shear UMAT and cohesive element approaches were independently run. While each captured portions of the response, both resulted in unrealistic responses. However, when these two methods were

combined, the result was the most accurate, consistent, and predictive correlation. It is important to note the significance of Table 5~~Table 5~~~~Table 4~~ in this regard. This table is a succinct evaluation of what to expect from the ~~vaious~~various models, and what needs to be improved for future work.

The results suggest these analytical approaches may be used to predict material response to possibly reduce material testing while also potentially supporting a probabilistic flaw framework. For this to be achieved, future work emphasized on scalability is necessary to be sure local defects are considered as part of entire structure. This requires development of a multi-scale approach which requires an understanding of flaw response when surrounded by unflawed material. Appropriate modelling of this response will allow for a better understanding of flaws on larger structures.

References

Abaqus Software and Abaqus Documentation: v. 6.12; Dassault Systemes Simulia Corp, Providence, RI, 2012.

Adams, D. O., and Bell, S. J.: Compression strength reductions in composite laminates due to multiple-layer waviness, Composites Sci. Tech., 53.2, 207-212, 1995.

Adams, D. O., and Hyer, M. W.: Effects of layer waviness on the compression strength of thermoplastic composite laminates, J. Reinforced Plastics and Composites, 12.4, 414-429, 1993.

Allen, D. H., and Searcy, C. R.: A micromechanical model for a viscoelastic cohesive zone, Int. J. Fracture, 107(2), 159-176, 2001.

Areias, P., and Belytschko, T.: Analysis of three-dimensional crack initiation and propagation using the extended finite element method, Int. J. Num. Methods in Eng., 63(5), 760-788, 2005.

Avery, D.P., Samborsky, D.D., Mandell, J.F. and Cairns, D.S.: Compression strength of carbon fiber laminates containing flaws with fiber waviness, Proc. of the 42nd AIAA, 54-63, 2004.

Baley, C., Davies, P., Grohens, Y., and Dolto, G.: Application of interlaminar tests to marine composites—A literature review, App. Composite Mater. 11.2, 99-126, 2004.

Barenblatt, G. I., The mathematical theory of equilibrium cracks in brittle fracture. Adv. in App. Mech., 7.1, 55-129, 1962.

Benzeggagh, M. L., and Kenane, M.: Measurement of mixed-mode delamination fracture toughness of unidirectional glass/epoxy composites with mixed-mode bending apparatus. Composites Sci. Tech., 56(4), 439-449, 1996.

Bouchard, P. O., Bay, F., Chastel, Y., and Tovena, I.: Crack propagation modelling using an advanced remeshing technique, Computer Methods in App. Mech. and Eng. 189(3), 723-742, 2000.

Blackketter, D. M., Walrath, D. E., and Hansen, A. C.: Modeling damage in a plain weave fabric-reinforced composite material, J. of Comp., Tech. and Res., 15.2, 136-142, 1993.

Cairns, D. S., Mandell, J. F., Scott, M. E., and Maccagnano, J. Z.: Design and manufacturing considerations for ply drops in composite structures. Composites Pt. B: Eng., 30.5, 523-534, 1999.

Camanho, P. P., and Matthews, F. L.: A progressive damage model for mechanically fastened joints in composite laminates, J. of Compo. Mater., 33.24, 2248-2280, 1999.

Camanho, P.P., Maimí, P., and Dávila, C.G.: Prediction of size effects in notched laminates using continuum damage mechanics, Comp. Sci. Tech., 67.13, 2715–2727, 2007.

Chaboche, J. L. A continuum damage theory with anisotropic and unilateral damage. La Recherche Aérospatiale, 2, 139-147, 1995.

Chang, F. K., and Chang, K. Y.: A progressive damage model for laminated composites containing stress concentrations, J. of Comp. Mat, 21(9), 834-855, 1987.

Chang, F. K., and Lessard, L. B.: Damage tolerance of laminated composites containing an open hole and subjected to compressive loadings: Part I—Analysis. J. of Compo. Mater., 25.1, 2-43, 1991.

Christensen R.M.: Stress based yield/failure criteria for fiber composites. Int. J. of Solids and Struct., 34.5, 529-43, 1997.

Costa, M.L., De Almeida, S., and Rezende, M.C.: Critical void content for polymer composite laminates, AIAA journal 43.6, 1336-1341, 2005.

Cui, Weicheng, and Wisnom, M. R.: A combined stress-based and fracture-mechanics-based model for predicting delamination in composites. Composites, 24.6, 467-474, 1993.

Daniel, I. M.: Failure of composite materials, Strain 43., 4-12 2007.

Dugdale, D. S.: Yielding of steel sheets containing slits, J. of the Mech. and Phy. of Sol., 8.2, 100-104, 1960.

Evcil, A.: Simulation of Three-Dimensional Progressive Damage in Composite Laminates, Intl. J. of Mech., 2, 2008.

Gorbatikh, L., Ivanov, D., Lomov, S., and Verpoest, I.: On modeling damage evolution in textile composites on meso-level via property degradation approach. Comp. Pt A, 38.12, 2433-2442, 2007.

Guo, Z. S., Liu, L., Zhang, B. M., and Du, S.: Critical void content for thermoset composite laminates. J. of Compo. Mater., 43.17, 1775-1790.

Hashin, Z.: Failure criteria for unidirectional fiber composites, J. of App. Mech., 47.2, 329-334, 1980.

Huang, H., and Talreja, R.: Effects of void geometry on elastic properties of unidirectional fiber reinforced composites. Compo. Sci. and Tech., 65.13, 1964-1981, 2005.

Icardi, U.: Assessment of recent theories for predicting failure of composite laminates, App. Mech. Rev., 60.2, 76-86, 2007.

Kachanov, L. M.: Introduction to continuum damage mechanics, Springer Netherlands, 1986. [Includes text of translation from Russian of: Kachanov, L. M.: On the creep fracture time. Izv Akad, Nauk USSR Otd Tech, 8, 26-31, 1958.]

Kerner, E. H.: The elastic and thermo-elastic properties of composite media, Proc. of Phys. Soc.. Section B 69.8, 808, 1956.

Krueger, R.: Virtual crack closure technique: history, approach, and applications, App. Mech. Rev., 57.2, 109-143, 2004.

Lemanski, S. L., Wang, J., Sutcliffe, M. P. F., Potter, K. D., & Wisnom, M. R.: Modelling failure of composite specimens with defects under compression loading, Comp. Pt. A: Appl. S., 48, 26-36, 2013.

Liu P.F. and Zheng J.Y.: Progressive failure analysis of carbon fiber/epoxy composite laminates using continuum damage mechanics, Mater. Sci. Eng. A., 485, 711–717, 2008.

Maimí, P., Camanho, P. P., Mayugo, J. A., and Dávila, C. G.: A continuum damage model for composite laminates: Part I–Constitutive model, Mech. of Mater., 39.10, 897-908, 2007.

Mandell, J. F., and Samborsky, D. D.: SNL/MSU/DOE June 25 2013 Composite Material Database, Version 22.0, 2013.

Moës, N., and Belytschko, T.: Extended finite element method for cohesive crack growth, Eng. Fract. Mech., 69.7, 813-833, 2002.

Nelson, J. W., Riddle, T. W., and Cairns, D. S.: Characterization and Mechanical Testing of Manufacturing Defects Common to Composite Wind Turbine Blades, Wind Energ. Sci. Discuss., doi:10.5194/wes-2017-13, in review, 2017.

Niu, K., and Talreja, R.: Modeling of wrinkling in sandwich panels under compression. J. Eng. Mech., 125.8, 875-883, 1999.

Paquette, J.: Blade Reliability Collaborative (BRC), Sandia National Laboratories, Wind Energy Technology Dept., 2012.

Petrossian, Z., and Wisnom, M.R.: Prediction of delamination initiation and growth from discontinuous plies using interface elements, Comp. Pt. A: Appl. S., 29.5, 503-515, 1998.

Pradeep, D., Reddy, N.J., Kumar, C.R., Srikanth, L., and Rao, R.M.V.G.K.: Studies on mechanical behavior of glass epoxy composites with induced defects and correlations with NDT characterization parameters, J. of Rein. Plast. and Compo., 26.15, 1539-1556, 2007.

Rice, J.: Elastic fracture mechanics concepts for interfacial cracks, J. Appl. Mech., 55.1, 98-103, 1988.

Sørensen, B. F., and Jacobsen, T. K., Determination of cohesive laws by the J integral approach, Eng. Fract. Mech., 70.14, 1841-1858, 2003.

Sosa J.C., Phaneendra, S., and Munoz, J.: Modelling of mixed damage on fibre reinforced composite laminates subjected to low velocity impact, Int. J. Damage Mech., 22.3, 1–19, 2012.

Su Z.C., Tay T.E., Ridha M., and Chen B.Y.: Progressive damage modeling of open-hole composite laminates under compression, Compos. Struct., 122, 507–517, 2015.

Talreja, R.: A continuum mechanics characterization of damage in composite materials, Proc. Roy. Soc. London A, 399, 1817, 1985.

Tay, T. E., Tan, V. B. C., and Tan, S. H. N.: Element-failure: an alternative to material property degradation method for progressive damage in composite structures. J. of Compo. Mater., 39.18, 1659-1675, 2005.

Tay, T. E., Tan, S. H. N., Tan, V. B. C., and Gosse, J. H.: Damage progression by the element-failure method (EFM) and strain invariant failure theory (SIFT), Compo. Sci. and Tech., 65.6, 935-944, 2005.

Tsai S.W.: Fundamental aspects of fiber reinforced plastic composites, Ann Arbor, MI: University Michigen Press. 1968.

Tsai, S. W., and Wu, E. M.: A general theory of strength for anisotropic materials. J. of Compo. Mater., 5.1, 58-80, 1971.

Turon, A., Davila, C. G., Camanho, P. P., and Costa, J.: An engineering solution for mesh size effects in the simulation of delamination using cohesive zone models, Eng. Fract. Mech, 74.10, 1665-1682, 2007.

Tvergaard, V., and Hutchinson, J. W.: Effect of strain-dependent cohesive zone model on predictions of crack growth resistance. Int. J. of Solids and Struct., 33, 3297-3308, 1996.

Van Paepegem, W., De Baere, I., and Degrieck, J.: Modelling the nonlinear shear stress–strain response of glass fibre-reinforced composites. Part I: Experimental results, Compo. Sci. and Tech., 66.10, 1455-1464, 2006.

Wang, J., Potter, K. D., Hazra, K., and Wisnom, M. R.: Experimental fabrication and characterization of out-of-plane fiber waviness in continuous fiber-reinforced composites, J. of Compo. Mater., 46.17, 2041-2053, 2012.

Wisnom, M.R., Reynolds, T., and Gwilliam, N.: Reduction in interlaminar shear strength by discrete and distributed voids, Compo. Sci. and Tech., 56.1, 93-101, 1996.

Wisnom, M. R., and Chang, F.K.: Modelling of splitting and delamination in notched cross-ply laminates, Compo. Sci. and Tech., 60.15, 2849-2856, 2000.

Zhu, H.Y., Li, D.H., Zhang, D.X., Wu, B.C., and Chen, Y.Y.: Influence of voids on interlaminar shear strength of carbon/epoxy fabric laminates, Trans. of Nonferrous Metals Soc. of China, 19, 470-5, 2009.